Modern optical potentials and the role of nuclear structure

S. Karataglidis

School of Physics, University of Melbourne, Victoria, 3010, Australia

Abstract. Microscopic descriptions of exotic nuclei are the subject of much experimental and theoretical effort. Not only are such important in their own right but are also necessary for applications in nuclear astrophysics. Evaluations of model wave functions may be done with analyses of elastic and inelastic scattering from hydrogen. Those require a realistic model of nucleon-nucleus scattering as scattering from hydrogen translates to proton scattering in the inverse kinematics. The Melbourne *g*-folding model for intermediate energy is presented along with various examples. Implications for existing and future experimental and theoretical work are discussed.

INTRODUCTION

The microscopic facets of the structures of exotic nuclei have been the subject of increased experimental and theoretical study, particularly with data now available for the scattering of heavy ions from hydrogen at intermediate energies. Such data are complementary to those obtained for breakup reactions, which only probe the asymptotic part of the initial state wave function of the exotic nucleus [1, 2]. Also, it has been established that the breakup of ^{6}He is a two-step process [3], with the final state interactions greatly influencing the reaction process. To investigate the wave functions of exotics at a deeper level one requires analyses of complementary scattering data.

In the absence of electron scattering data, intermediate-energy proton scattering represents the best probe of the microscopic structures of exotic nuclei. This was illustrated by Karataglidis *et al.* who compared electron and proton elastic and inelastic scattering from ^{12}C [4] and ^{6,7}Li [5]. They found that the behaviour with momentum transfer of the form factors from electron scattering was found also in the differential cross sections from intermediate energy proton scattering, reflecting the deficiencies in the wave functions from the underlying assumed model structure. Such comparisons were only possible when credible models of scattering for both electrons and protons from nuclei were specified.

It is well-known that few-body descriptions of exotics, especially the halo nuclei, are able to describe breakup reactions as those models are able to give the correct asymptotic behaviour of the wave functions. A problem, however, exists when attempting to use such wave functions in descriptions of scattering from hydrogen: a credible description of the structure of the core is necessary to account for the full density, which is required to analyse nucleon scattering data. That was found in analyses of scattering from ^{9}Li and ^{11}Li [6]. More recently, such models incorporating multiple scattering expansions of the nucleon-nucleon (*NN*) scattering amplitudes [7, 8] have sought to describe proton

scattering from halos using few-body models. However, predictions from those models are still prone to significant changes arising from problems in specifying the density of the core [7]. At intermediate energies, medium modifications are essential in the specification of the *NA* optical potential (OMP) and the multiple scattering expansions, taken to second order [7], are only a gross approximation. A full *g*-matrix specification of the optical potential is needed to account for those corrections [9].

As microscopic models of the nucleon-nucleus (*NA*) optical potentials are based on effective *NN* interactions, these problems are overcome when models of structure which admit nucleon degrees of freedom are used. Herein, a description of the Melbourne optical potential [9] which accounts for scattering from both stable and exotic nuclei self-consistently is presented. That model has been used successfully with the shell model [9], Skyrme-Hartree-Fock (SHF) models [10], and the RPA [11, 12]. After giving a brief description of the model, various results are given with a view to future experiments which may be done at radioactive beam facilities. Concluding remarks follow.

THE G-FOLDING OPTICAL MODEL - MELBOURNE FORCE

The Melbourne force is discussed in detail in a recent review article by Amos *et al.* [9], to which the reader is referred. A brief overview of the model is presented herein with emphasis on how structure enters into the description of elastic and inelastic scattering.

The optical potential for *NA* scattering is associated with the elastic scattering channel. Following the Feshbach formalism [13], we split the Hilbert space into the elastic scattering channel (P space) and non-elastic channels (Q space). The Schrödinger equation then becomes, with P and Q projectors onto the respective spaces

$$\begin{aligned} (E-H_{PP})\left|\Psi^{(+)}\right\rangle &= H_{PQ}\left|\Psi^{(+)}\right\rangle \\ (E-H_{QQ})\left|\Psi^{(+)}\right\rangle &= H_{QP}\left|\Psi^{(+)}\right\rangle , \end{aligned} \tag{1}$$

where $H_{XY} = XHY$. Recoupling, and taking the one-body approximation gives the Schrödinger equation for the projectile wave function, *viz.*

$$\left\{E-H_0-\left\langle\Phi_{gs}\left|V\right|\Phi_{gs}\right\rangle-\left\langle\Phi_{gs}\left|VG_{QQ}^{(+)}V\right|\Phi_{gs}\right\rangle\right\}\left|\chi^{+}\right\rangle = 0 \tag{2}$$

where $G_{QQ}^{(+)} = [E-H_{QQ}+i\varepsilon]^{-1}$, from which the optical potential is defined as

$$U = \left\langle\Phi_{gs}\left|V\right|\Phi_{gs}\right\rangle+\left\langle\Phi_{gs}\left|VG_{QQ}^{(+)}V\right|\Phi_{gs}\right\rangle . \tag{3}$$

Specification of the optical potential is a many-body problem with explicit dependence on the target ground state wave function. It is complex, nonlocal and energy dependent, through V and also $G_{QQ}^{(+)}$. The second term is the Dynamic Polarising Potential

(DPP) and defines how coupling to nonelastic channels varies with energy. Specifically, such coupling may be cast into three energy regimes:

Low energy For $E < 10$ MeV, explicit coupling to specified, discrete low-lying excited states of the target is necessary. A recent development in the construction of such models is the Multi-Channel Algebraic Scattering theory [14, 15] which is the subject of another presentation at this meeting [16];

Giant resonances Between 10 and 25 MeV coupling to the giant resonances becomes important [17]. One important exception are the He isotopes, for which there are no giant resonances;

Intermediate and High energies At higher energies and as the level density becomes high, coupling to excited states may be handled implicitly by using folding models based on the *NN* g matrices for infinite matter.

An example of the last is the Melbourne g-folding model [9]. The model takes as its basis an effective *NN* interaction obtained from the g matrices of the bare *NN* interaction. For an incident nucleon, momentum $\mathbf{p}_0$ in collision with a nucleon embedded in infinite matter with momentum $\mathbf{p}_1$, those g matrices are solutions of the Bruckner-Bethe-Goldstone equation in momentum space, *viz.*

$$g(\mathbf{q},\mathbf{q}';\mathbf{K}) = V(\mathbf{q},\mathbf{q}') + \int V(\mathbf{q}',\mathbf{k}')\frac{Q(\mathbf{k}',\mathbf{K};k_f)}{[E(\mathbf{k},\mathbf{K}) - E(\mathbf{k}',\mathbf{K})]}g(\mathbf{k}',\mathbf{q};\mathbf{K})\,d\mathbf{k}', \qquad (4)$$

where $\mathbf{k} = (\mathbf{p}_0 - \mathbf{p}_1)$ is the relative momentum and $\mathbf{K}$ is the centre-of-momentum of the two particles. Primes denote the equivalent set of momenta after scattering. Q is a Pauli-blocking operator and the energies E in the propagator contain auxiliary potentials which model the effects of the nuclear medium [18]. As Q and energies E are dependent on $\mathbf{k}'$, in practice they are replaced by their angle-averaged values. This has been shown to be a good approximation for nuclear densities above $\sim 15\%$ [19, 20], and is an important consideration for scattering from exotic nuclei where scattering is observed as from the core in the case of halo nuclei [21].

Once the g matrices in infinite matter are obtained, they are mapped to those for finite nuclei in coordinate space [9] by folding in the specified (model) density of the target. The mapping to coordinate space is achieved by means of a double Bessel transform and allows for the explicit specification of central, tensor, and two-body spin-orbit terms as sums of Yukawa functions. (This is also a practical consideration: the DWBA suite of programs [22] which are used to calculate observables require a coordinate space representation of the potential.) Once these effective g matrices (g_{eff}) have been obtained, the nonlocal, complex, OMP for scattering is defined as

$$\begin{aligned} U(\mathbf{r},\mathbf{r}';E) &= \delta(\mathbf{r}-\mathbf{r}')\sum_i n_i \int \varphi_i^*(\mathbf{s}) g_D(\mathbf{r},\mathbf{s};E)\varphi_i(\mathbf{s})\,d\mathbf{s} \\ &\quad + \sum_i n_i \varphi_i(\mathbf{r}') g_E(\mathbf{r},\mathbf{r}';E)\varphi_i \\ &= U_D(\mathbf{r},E)\delta(\mathbf{r}-\mathbf{r}') + U_E(\mathbf{r},\mathbf{r}';E) \end{aligned} \qquad (5)$$

where D and E denote the direct and exchange terms of the effective interaction respectively. Nuclear structure information enters via the occupation numbers n_i for each orbit

i. The direct term is the well-known $g\rho$ form of the optical potential and is local. The nonlocality arises from the explicit exchange terms; neglecting such terms can lead to serious problems [23]. A credible model of structure is necessary in the specification of the optical potential.

The single particle wave functions entering in Eq. (5) are usually assumed to be of harmonic oscillator (HO) form. For most nuclei this is a reasonable assumption and is consistent with the underlying shell model. However, for halo nuclei it is more appropriate to use Woods-Saxon (WS) wave functions [21] with binding energies of the orbits occupied by the halo set to the separation energy of the single nucleon in the halo.

Inelastic scattering may be calculated in a distorted-wave approximation (DWA) with the g_{eff} as the operators effecting the transition. The transition amplitude may be written, with '0' and '1' denoting the projectile and bound state nucleon, respectively, as

$$T_{J_f J_i}^{M_f M_i \nu' \nu}(\theta) = \left\langle \chi_{\nu'}^{(-)}(0) \right| \left\langle \Psi_{J_f M_f} \left| A g_{\rm eff}(0,1) \mathscr{A}_{01} \right| \Psi_{J_i M_i} \right\rangle \left| \chi_{\nu}^{(+)}(0) \right\rangle \Big\} \ . \tag{6}$$

In Eq. (6), the distorted wave function for the projectile is denoted by χ, and $\mathscr{A}_{01}$ is the antisymmetrization operator for the projectile and bound state nucleon. For a spin-zero target, one obtains after expanding the many-body wave function

$$\begin{aligned} T_{J_f J_i}^{M_f M_i \nu' \nu}(\theta) &= \sum_{\alpha_1 m_1 \alpha_2 m_2} \frac{(-1)^{j_1 - m_1}}{\sqrt{2J_f+1}} \langle j_2 m_2 \, j_1 \, -m_1 \, | J_f M_f \rangle \left\langle J_f \left\| \left[a_{\alpha_2}^{\dagger} \times \tilde{a}_{\alpha_1} \right]^{J_f} \right\| 0 \right\rangle \\ &\times \left\langle \chi_{\nu'}^{(-)}(0) \right| \left\langle \varphi_{\alpha_2}(1) \left| A g_{\rm eff}(0,1) \mathscr{A}_{01} \right| \varphi_{\alpha_1}(1) \right\rangle \left| \chi_{\nu}^{(+)}(0) \right\rangle \Big\} \ , \end{aligned} \tag{7}$$

where $\alpha = \{l, m, j\}$.

NUCLEAR STRUCTURE FACETS

The optical model potential in the *g*-folding model is a one-body operator with respect to the target (bound) nucleons, and so one requires specification of the one-body density matrix elements (OBDME), *viz.*

$$S_{\alpha_1 \alpha_2 J} = \left\langle J_f \left\| \left[a_{\alpha_2}^{\dagger} \times \tilde{a}_{\alpha_1} \right]^{J} \right\| J_i \right\rangle \ . \tag{8}$$

Various models have been utilised but, for the most part, the shell model has been used to specify the OBDME. Others include the Skyrme-Hartree-Fock (SHF) and the RPA, results from both of which are presented below. Note that in specifying the OMP one must keep to the level of the density matrix *elements* as that preserves the nonlocality. Use of the density itself requires gross approximations to be made in the handling of the nonlocal exchange terms. That may be problematic [23].

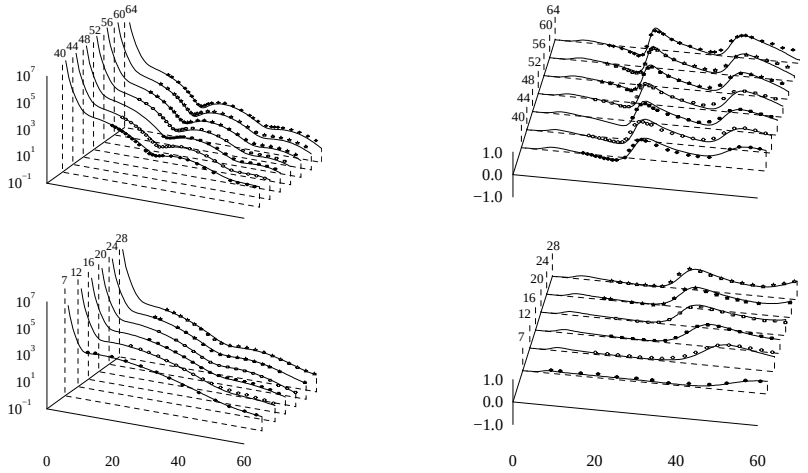

FIGURE 1. Differential cross sections (left) and analysing powers (right) for the elastic scattering of 65 MeV protons from various nuclei to mass 64.

RESULTS

The BonnB *NN* interaction was used to obtain the g_{eff} for all results presented herein. All results were obtain using DWBA98 [22] from single-shot calculations; there was no fitting to data. The review [9] present most results obtained up to that time, and includes a discussion on the connection between electron and proton scattering. A subset of those results are discussed below, as well as those obtained since the review.

Systematic analyses of elastic scattering across the mass range, and for several energies, have been reported (see, eg., [9]). Results of analyses of elastic scattering differential cross sections and analysing powers for the scattering of 65 MeV protons from nuclei up to mass-64 are presented in Fig. 1. Clearly the differential cross sections and analysing powers at 65 MeV are well reproduced by the model. Of particular note is the excellent reproduction of the observables' dependence with momentum transfer as one increases the mass.

Fig. 2 displays the differential cross section for the elastic scattering of ^{6}He ions from hydrogen at 41*A* MeV (data of Lagoyannis *et al.* [24]) as well as the inelastic scattering cross section to the 2^{+} state. The use of WS functions, depicted by the solid line, to specify the density of ^{6}He as consistent with a neutron halo gives better agreement with the elastic scattering data. (The results using HO functions are given by the dashed lines.) At these energies, the proton does not observe the halo directly but rather its effect in depleting the neutron density in the core to the halo. The effect is observed as a decrease in the differential cross section at large angles. As $E2$ transitions are surface-peaked, the halo is better illustrated in the inelastic scattering to the 2^{+} state as an enhancement in the cross section around 30°.

The SHF model has been used to describe systematic behaviour in exotic nuclei as one approaches the drip lines. One may evaluate the wave functions obtained therefrom in analyses of reaction cross section data. We compare the results of calculations made

at 65 and 200 MeV using SHF wave functions with the SkX* force [25] in Fig. 3 with estimates by Carlson [26]. The level of agreement is quite good and the calculations exhibit the Coulomb shift, which is more pronounced at 65 MeV. Of note is that as one increases neutron number one moves away from the line of minimal isospin.

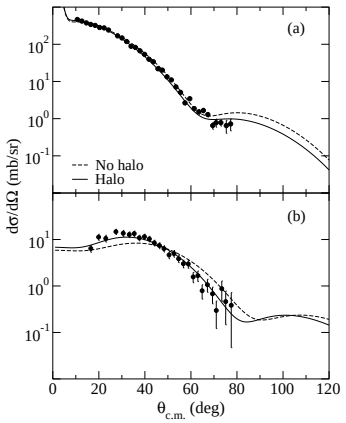

FIGURE 2. Differential cross sections for the elastic and inelastic scattering of ^{6}He from hydrogen.

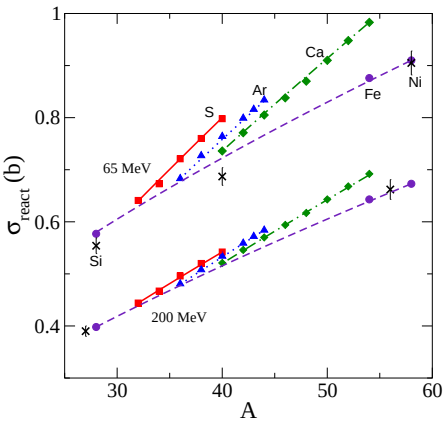

FIGURE 3. Reaction cross sections for S, Ar, and Ca isotopes at 65 and 200 MeV.

This illustrates a possible signature for exotic structures.

Fig. 4 shows the proton and neutron densities for the Sn isotopes from ^{100}Sn to

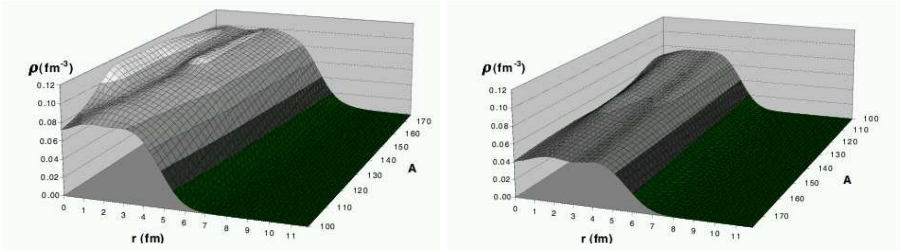

FIGURE 4. Neutron (left) and proton (right) densities for the Sn isotopes from the SHF model.

^{168}Sn as obtained from an SHF model using the SLy4 force [27]. Those densities exhibit various structures as one increases mass, notably an indication of neutron halos around $A = 150$. Fig. 5 shows the differential cross sections and polarisations for a sample of Sn isotopes as compared to data at 40 MeV. The level of agreement between the results and data is reasonable and extends naturally to the variation with mass.

Fig. 6 displays the results for elastic and inelastic proton scattering from ^{208}Pb [12], at 121 and 135 MeV, respectively. The RPA model was used to obtain the ground state and transition densities as required. The elastic scattering cross section data [28] are also compared to the results of an SHF calculation using the SkM* force [10]. The agreement with data illustrates that both the SHF and RPA models for ^{208}Pb for the ground state are reasonable. Of the two models, only the RPA may be able to specify transitions densities and those have been used to obtain the results of the inelastic scattering. Data [29] and results for the transitions to the 2^+ and 3^- states are compared in the right panel of Fig. 6. Use of the RPA allows for a self-consistent analysis of data leading to the even and odd parity states in ^{208}Pb. That both sets of results are out of phase with respect to

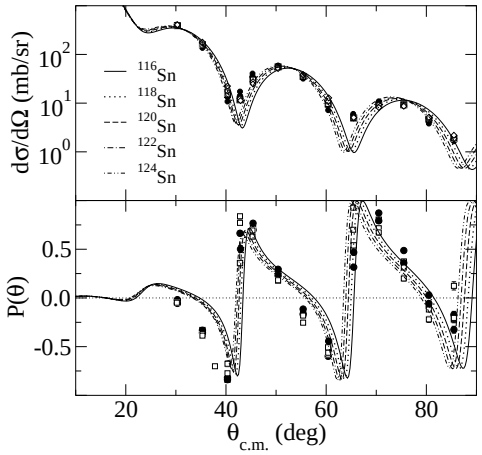

FIGURE 5. Differential cross sections and polarisations for 40 MeV proton scattering from a sample of Sn isotopes.

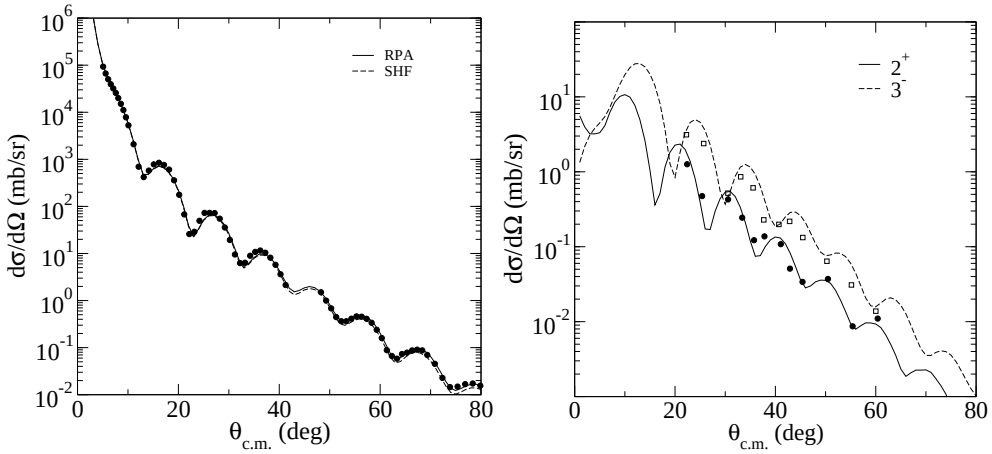

FIGURE 6. Differential cross section for 121 MeV elastic (left) and 135 MeV inelastic (right) proton scattering from ^{208}Pb.

each other is consistent with the phase rule of Blair [30].

CONCLUSIONS

We have presented a predictive model of nucleon-nucleus scattering at intermediate energies for which nuclear structure plays a central part. As such it is most appropriate for eliciting structure information of exotic nuclei from analyses of scattering of beams from hydrogen. Such analyses are complementary to electron scattering which, given the absence of electron scattering data, makes scattering from hydrogen the best (current) means of understanding exotic nuclei at a microscopic level.

The model has been tested by analyses of proton scattering data across the mass

range and for various energies. For light nuclei, use of the shell model with appropriate choices of single particle wave functions allows for analyses of data out to the drip lines. Extension of such analyses to heavy nuclei is achieved by use of the Skyrme-Hartree-Fock and RPA models. In all cases, the underlying proton scattering model is consistent; analyses is predicated on a credible choice of structure model for the target.

It is hoped that facilities utilising exotic beams continue scattering experiments with hydrogen as the target, to allow for a deeper understanding of the structures of nuclei out to the drip lines. Such experiments are not restricted to intermediate energies, for which the Melbourne force is appropriate. With the advent of a Multi-Channel Algebraic Scattering theory (see [16], this conference) analyses of data from low-energy facilities may be done with the same predictive power.

REFERENCES

1. Hansen, P. G., *Phys. Rev. Lett.*, **77**, 1016 (1996).
2. Esbensen, H., *Phys. Rev. C*, **53**, 2007 (1996).
3. Aleksandrov, D., et al., *Nucl. Phys.*, **A633**, 234 (1998).
4. Karataglidis, S., Dortmans, P. J., Amos, K., and de Swiniarski, R., *Phys. Rev. C*, **52**, 861 (1995).
5. Karataglidis, S., Brown, B. A., Amos, K., and Dortmans, P. J., *Phys. Rev. C*, **55**, 2826 (1997).
6. Crespo, R., Tostevin, J. A., and Thompson, I. J., *Phys. Rev. C*, **54**, 1867 (1996).
7. Crespo, R., and Johnson, R. C., *Phys. Rev. C*, **60**, 034007 (1999).
8. Crespo, R., Thompson, I. J., and Korsheninnikov, A. A., *Phys. Rev. C*, **66**, 021002(R) (2002).
9. Amos, K., Dortmans, P. J., von Geramb, H. V., Karataglidis, S., and Raynal, J., *Adv. Nucl. Phys.*, **25**, 275 (2000).
10. Karataglidis, S., Amos, K., Brown, B. A., and Deb, P. K., *Phys. Rev. C*, **65**, 044306 (2002).
11. Dupuis, M., Karataglidis, S., Bauge, E., Delaroche, J.-P., and Gogny, D. (2005), nucl-th/0504013.
12. Dupuis, M., Karataglidis, S., Bauge, E., Delaroche, J.-P., and Gogny, D. (2005), nucl-th/0506077.
13. Feshbach, H., *Ann. Phys. (N.Y.)*, **19**, 287 (1962).
14. Amos, K., Canton, L., Pisent, G., Svenne, J. P., and van der Knijff, D., *Nucl. Phys.*, **A728**, 65 (2003).
15. Canton, L., Pisent, G., Svenne, J. P., van der Knijff, D., Amos, K., and Karataglidis, S., *Phys. Rev. Lett.*, **94**, 122503 (2005).
16. Amos, K. (2005), presentation at this conference.
17. von Geramb, H. V., et al., *Phys. Rev. C*, **12**, 1697 (1975).
18. Haftel, M., and Tabakin, F., *Nucl. Phys.*, **A158**, 1 (1970).
19. Legindgaard, W., *Nucl. Phys.*, **A297**, 429 (1978).
20. Cheon, T., and Redish, E. F., *Phys. Rev. C*, **39**, 331 (1989).
21. Karataglidis, S., Dortmans, P. J., Amos, K., and Bennhold, C., *Phys. Rev. C*, **61**, 024319 (2000).
22. Raynal, J., computer program dwba98, nea 1209/05 (1998).
23. Deb, P. K., and Amos, K., *Phys. Rev. C*, **62**, 024605 (2000).
24. Lagoyannis, A., et al., *Phys. Lett.*, **B518**, 27 (2001).
25. Brown, B. A., Richter, W. A., and Lindsay, R., *Phys. Lett.*, **B483**, 49 (2000).
26. Carlson, R. F., *Atom. Data and Nucl. Data Tables*, **63**, 93 (1996).
27. Amos, K., Karataglidis, S., and Dobaczewski, J., *Phys. Rev. C*, **70**, 024607 (2004).
28. Nadasen, A., et al., *Phys. Rev. C*, **23**, 1023 (1981).
29. Adams, G. S., et al., *Phys. Lett.*, **91B**, 23 (1980).
30. Amos, K. A., McCarthy, I. E., and Greider, K. R., *Nucl. Phys.*, **68**, 469 (1965).